Title

Hyperlocal environmental heterogeneity at restored rocky intertidal and salt marsh habitats at Gansevoort Peninsula: Implications for urban restoration of shallow coastal habitats in New York City

Authors

James J. Herlan, Adelia H. Harrison, John Paul Hellenbrand, Nikhita Kannam, Andrew Reinmann, Ricardo Toledo-Crow & Phillip P.A. Staniczenko

Abstract

Hudson River Park Trust (HRPT) is a steward for more than 550 acres of park land and water in one of North America's densest urban areas, New York City. Accordingly, HRPT seeks to enhance wetland and nearshore habitat within Park boundaries (ESMP Research & Habitat Enhancement Goal 2) by restoring oyster reefs (eastern oyster, *Crassostrea virginica*) and salt marshes containing cord grass (*Spartina alterniflora*). While sedimentation and pollution associated with agriculture and urbanization have been shown to impact the health of oyster reefs and salt marshes, there are few studies on the role that water motion has on oyster and cord grass growth and survival and therefore restoration success. To address this knowledge gap, we examined the hyperlocal environmental heterogeneity of water velocity (cm s^{-1}) (a proxy for *wave exposure*) and temperature (°C) at Gansevoort Peninsula. We are currently analyzing biological data on cord grass in the salt marsh habitat and provide initial results on the relationship between the rocky intertidal habitat hyperlocal environment and the survival and growth of oyster spat (*Crassostrea virginica*). Our results show a significant difference in the overall mean velocity (cm s^{-1}) between an eastern location, with a higher mean velocity of 7.06 cm s^{-1}, compared to an western location, with a lower mean velocity of 4.60 cm s^{-1}. Overall, the mean water temperature was similar (around 23.5°C) at eastern and western locations. At the salt marsh, we found significant hyperlocal differences in mean water velocity (cm s^{-1}) and temperature (°C) spatially (across the width of a rectangular plot) and temporally (October to December 2024). As expected, water temperatures increased (°C) from late Winter through early Spring (March to May 2025). Lastly, we investigated if the use of high tide ranges predicted by NOAA were appropriate to assume total submergence of the velocity meters at the saltmarsh. To accurately analyze unbiased data of water velocity (cm s^{-1}) (i.e., measurements not biased by meter tilt due to exposure at low tide), we explored the relationship between water velocity (cm s^{-1}) and water level (m) using data collected from water level meters. Our results yielded a steep decline in water velocity (cm s^{-1}) at 0.18 m and estimated a critical threshold at 0.20 m. To better understand the relationship between water velocity (cm s^{-1}) and tides, we recommend pairing water velocity and level meters in the salt marsh to identify localized flooding and submergence cycles of salt marsh relative to predicted NOAA tidal cycles. Our study enhances the environmental and hydrological data collected through the Hudson River Ecosystem Conditions Observing System (HRECOS) and provides valuable information

for Park managers on selecting locations for oyster spat placement at restoration sites. This project provides actionable evidence for optimizing oyster and salt marsh restoration programs at Gansevoort Peninsula and similar nearshore urban restoration habitats.

Introduction

The ecology, biodiversity, and ecosystem functioning of oyster reef and salt marsh communities are affected by the physical forcings caused by surface winds and current flow, together defined as *wave exposure* (Massel 1999; Denny and Gaylord 2010). The degree of wave exposure can either enhance growth by delivering food and nutrients or hinder growth by inducing physiological stress and physical damage (e.g., dislodgement, displacement, mortality; Sousa 1984; Lenihan and Peterson 1998). Due to the loss of submerged oyster reef structures, Hudson River coastlines have experienced increased wave exposure and sedimentation (Brandon et al. 2016). Nevertheless, studies have shown that oysters can grow and survive in natural yet highly urbanized estuaries and salt marshes, such as those in nearby Jamaica Bay (Zarnoch & Schreibman 2012). Given the many benefits provided by urban oyster reefs, it is imperative decision-makers understand how anthropogenic change is impacting reef ecology, so that nature-based solutions such as oyster reef restoration can be optimized. While research has begun to identify human-influenced abiotic factors that suppress oyster development, such as elevated sedimentation loads and heavy metals concentrations (Fitzgerald et al. 2020), no study has investigated the effects of hyperlocal differences in wave exposure that might exist in highly altered urban environments.

Wetlands are an additional habitat type located at the transition between land and shallow water, where terrestrial and aquatic ecosystems meet and interact (Cowardin et al. 1979). For most of the last century, wetland ecosystems were mainly impacted by agricultural and urban expansion, through eutrophication, species invasions, and pollution (Zedler and Kercher 2005). More recently, atypical weather events have emerged as a prominent driver of decreasing wetland health, leading to dramatic reductions in wetland ecosystem services such as biodiversity support, water quality enhancement and filtration, flood abatement, and carbon sequestration (Feagin et al. 2009). One type of wetland that has been particularly impacted by atypical weather events is salt marshes, which have experienced increasing saltwater intrusion and flooding from accelerating sea level rise and more frequent storms (*ibid*). An important environmental factor that affects salt marsh ecology is wave exposure. As salt marshes erode, the corresponding increase in open water creates more favorable conditions for generating larger waves, which results in a damaging positive feedback cycle that leads to further wetland erosion (Denny 1988; Karimpour et al. 2017). While the physical process of wind-driven wave erosion is well understood, the implications for wetland restoration is not.

For this study, we examined the hyperlocal environmental heterogeneity of water velocity (cm s^{-1}) (a proxy for *wave exposure*) and temperature (°C) at Gansevoort Peninsula. We tested four hypotheses: (i) there is no difference in water velocity (cm s^{-1}) and temperature (°C) between eastern and western locations at the rocky intertidal

habitat at Gansevoort Peninsula; (ii) there is no difference in water velocity (cm s^{-1}) and temperature (°C) along the narrow width of the of the salt marsh habitat plot at Gansevoort Peninsula; (iii) there is no difference in water velocity (cm s^{-1}) and temperature (°C) at the salt marsh habitat through Summer, Autumn, and Winter 2024; and(iv) there is no difference in water velocity (cm s^{-1}) and temperature (°C) at the salt marsh habitat during the late winter and early Spring 2025.

Methods

We deployed two tilt current meters (TCM-4 Shallow Water Tilt Current Meter from Lowell Instruments, LLC) along Gansevoort Peninsula's northern rocky shoreline at an eastern (closer to Hudson River Park's esplanade) and western (closer to the Hudson River's main channel) location (Figs. 1 and 2) during Summer and Fall 2024 and Winter and Spring 2025.

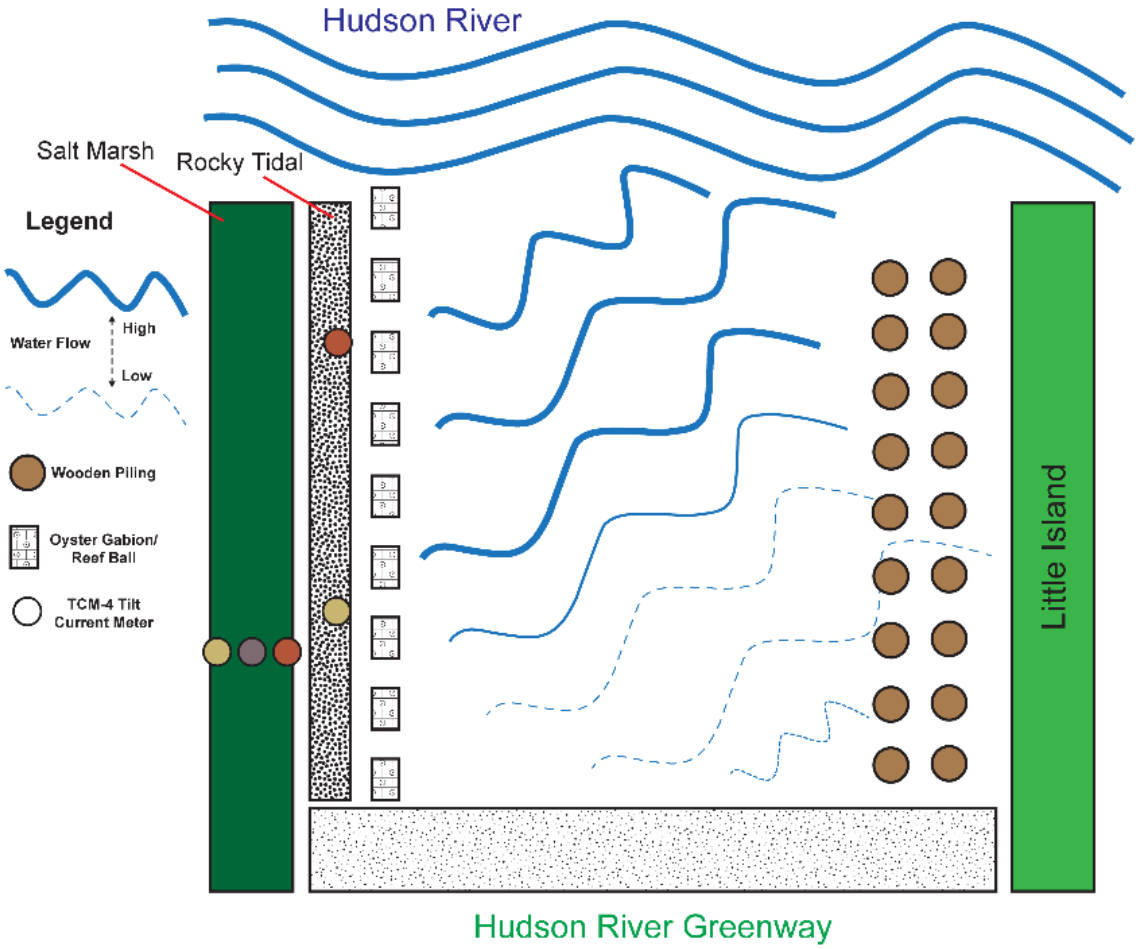

Figure 1. Gansevoort Peninsula Rocky Intertidal. Map of Gansevoort Peninsula, Manhattan (NYC); eastern and western locations of current meters and oyster spat reef balls are shown.

Figure 2. Photograph of study site at Gansevoort Peninsula as viewed facing west and showing the locations of the offshore and inshore meters along the rocky intertidal in July and August.

Between October and December 2024, we transferred the current meters and redeployed them to the salt marsh habitat at Gansevoort Peninsula at three locations that spanned the width of the western portion of the salt marsh plot: inshore (i.e., near the Peninsula's northern walkway), midshore (i.e., center of salt marsh plot), and offshore (nearest to the rocky intertidal habitat) (Figs. 1, 3, and 4). TCM-4 meters are engineered to measure current speed (mean velocity, cm s^{-1}) based on the *drag-tilt principle* (Fig. 5).

Figure 3. Photograph of salt marsh study site at Gansevoort Peninsula showing inshore, midshore, and offshore locations of current meters within the salt marsh habitat.

Figure 4. Photographs of salt marsh study site from Summer to Winter 2024.

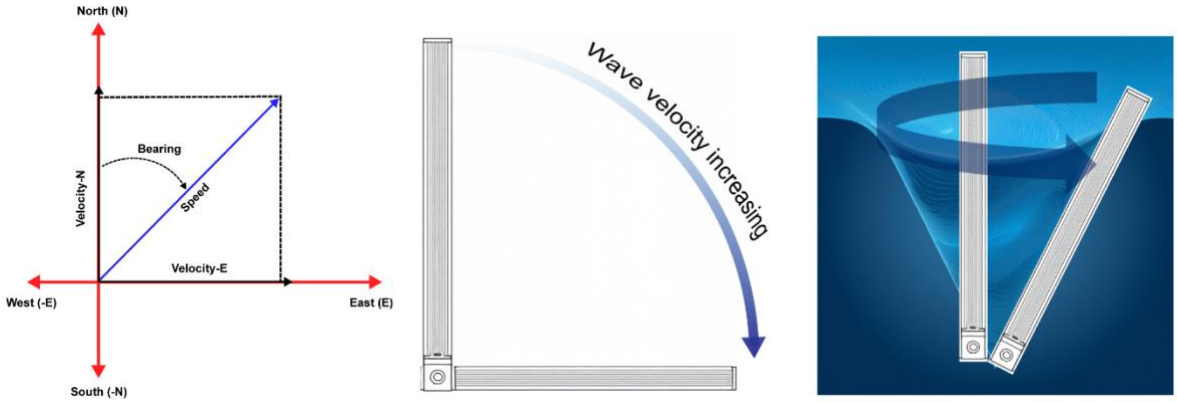

Figure 5. TCM-4 meters are engineered to measure current speed (mean velocity, cm s^{-1}) based on the drag-tilt principle. Adapted from pages 22 and 43 of the *Universal User Guide for TCM-x Current Meters, MAT-1 Data Logger, and Domino Software*. © 2014–2022 Lowell Instruments, LLC.

The meters were positively buoyant during high tidal ranges and anchored to a concrete slab using an embedded PVC-coupling with a short rope tether. Drag from the moving water of the Hudson River would tilt the meter in the direction of water flow, while the meter's accelerometer and magnetometer recorded the amount and direction of tilt, respectively, to calculate mean velocity (cm s^{-1}) per sampling interval. Meters were configured to a 15-minute sampling interval and 15-minute burst interval with a rate of 8 Hz for 20-second burst durations. Field sampling consisted of retrieving the meters and downloading data files to a laptop computer between June 19 and September 18, 2024 at the rocky intertidal habitat, and then between October 11 and December 19, 2024 at the salt marsh habitat (Fig. 6). We recorded data as water velocity (cm s^{-1}) and temperature (°C); daily and overall mean water velocities (cm s^{-1}) were summarized using high tide measurements (± 3 hours) referenced from NOAA Tides and Currents using data recorded in the Battery (Station ID: 8518750).

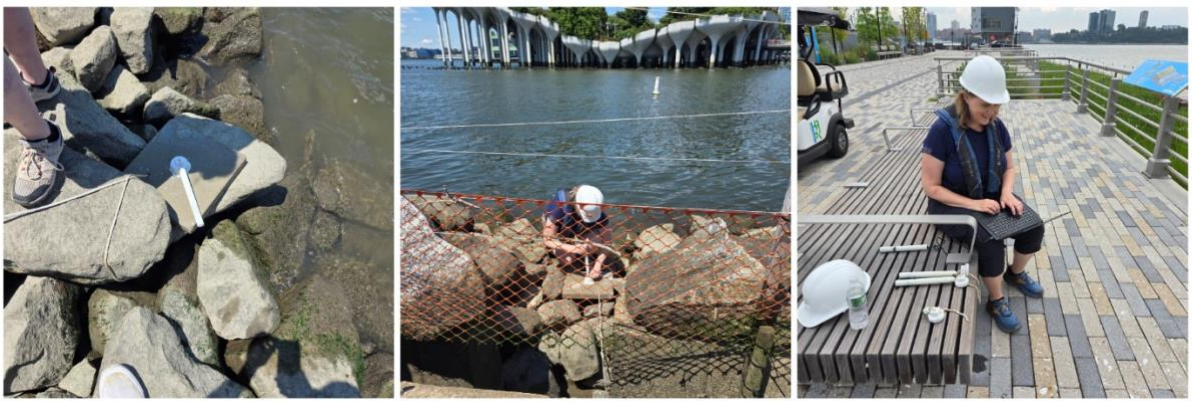

Figure 6. TCM-4 Current Meter (Lowell Instruments, LLC) deployment, retrieval, and data download.

Statistical analysis

We used the statistical programming language R 4.4.2 (R Team 2025) and nonparametric Mann-Whitney *U*-tests to compare eastern and western locations at rocky intertidal habitat groups, and Kruskal-Wallis tests to compare inshore, midshore, and offshore locations at salt marsh habitat because the assumption of independent, identically distributed, and normally distributed residuals was violated.

Results

Rocky intertidal habitat

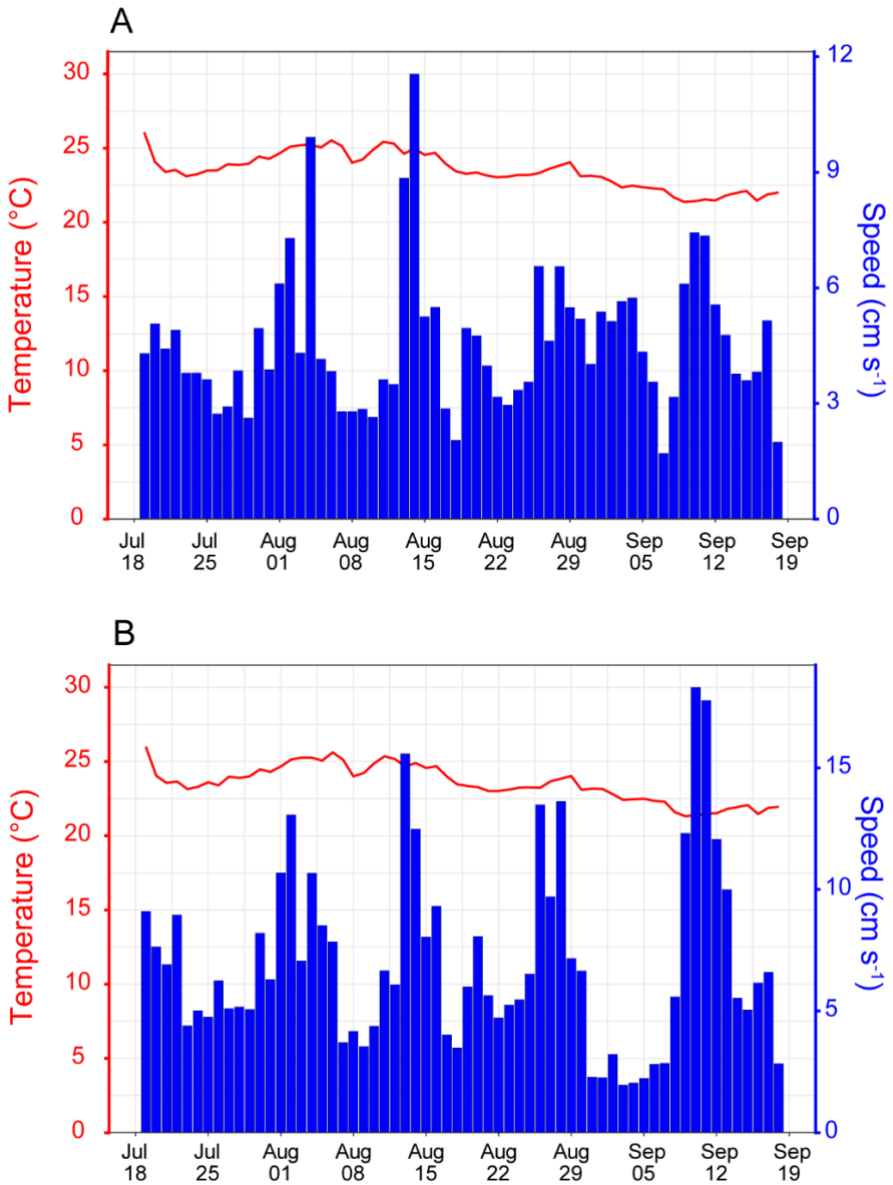

Figure 7. Mean daily water velocities (cm s^{-1}) and temperatures (°C) at the eastern (Panel A) and western locations (Panel B).

	Mean Daily Velocity (cm s^{-1})	Mean Daily Temperature (°C)	Point-sample water velocity (cm s^{-1})	Point-sample Temperature (°C)	Overall Mean Velocity (cm s^{-1})	Overall Mean Temperature (°C)
East	1.71 ± 2.58 to 11.6 ± 36.5	21.5 to 26	0 to 227	20 to 26	4.60 ± 17.5	23.5 ± 1.3
West	1.96 ± 1.56 to 18.3 ± 36.77	21.5 to 26	0 to 243	20 to 26	7.06 ± 10.2	23.5 ± 1.3

Table 1. Rocky Intertidal – Gansevoort Peninsula. Ranges and means with standard deviations of water properties at the east and west meter locations.

Our results show that the difference in the overall mean velocity (cm s^{-1}) between the two rocky intertidal locations (Fig. 7) was significant ($W = 4 \times 10^6$, $p < 0.001$), with a higher mean velocity (cm s^{-1}) at the western location closer to the Hudson River's main channel, compared to the eastern location closer to the esplanade (Table 1; Fig. 8).

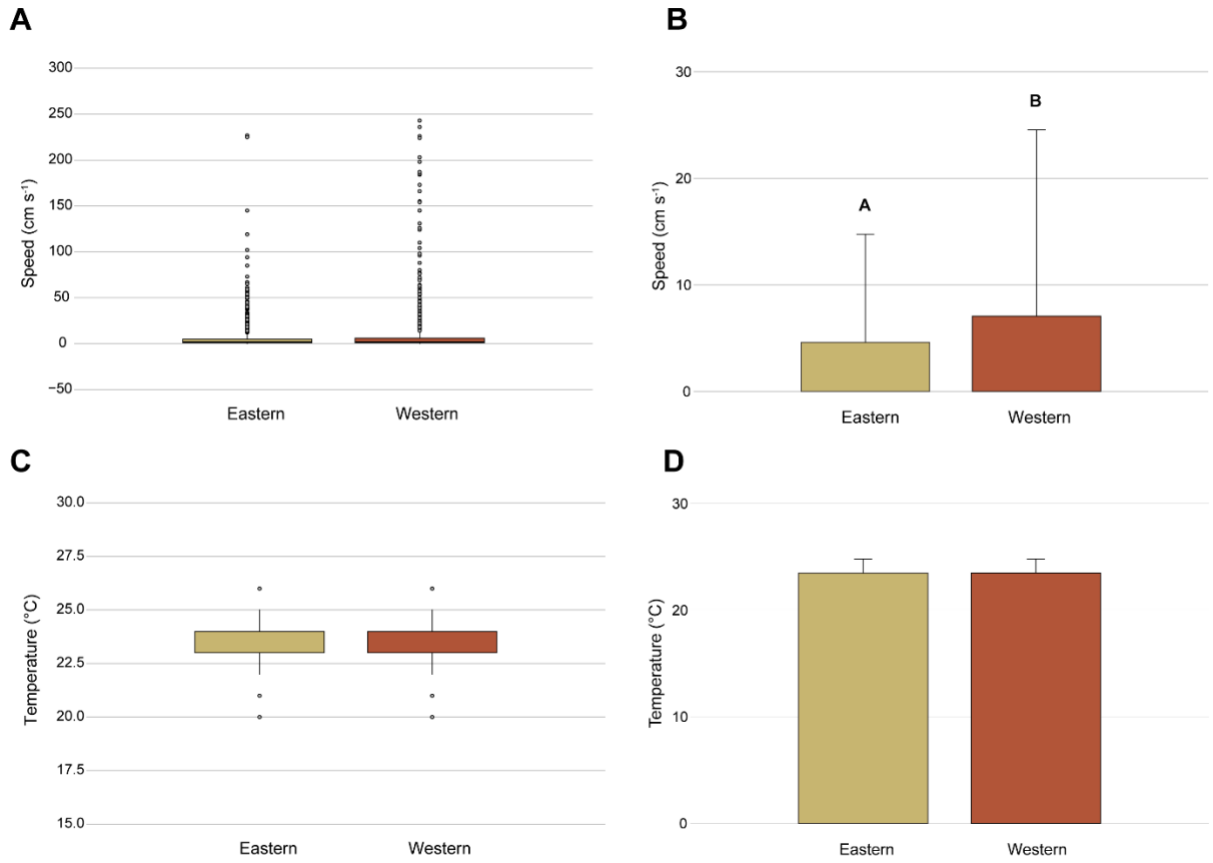

Figure 8. Rocky Intertidal – Gansevoort Peninsula (Panels A & C). Box-and-whisker plots showing the upper and lower adjacent values of the smallest and largest water velocity (cm s^{-1}) and temperature (°C) observations within the range (median – 1.5 IQR, median + 1.5 IQR), where IQR is the interquartile range; outlying values are all individual observations outside the range of adjacent values (Panels B & D). Overall mean water velocity (cm s^{-1}) and temperature (°C); error bars are standard deviation.

Salt marsh habitat

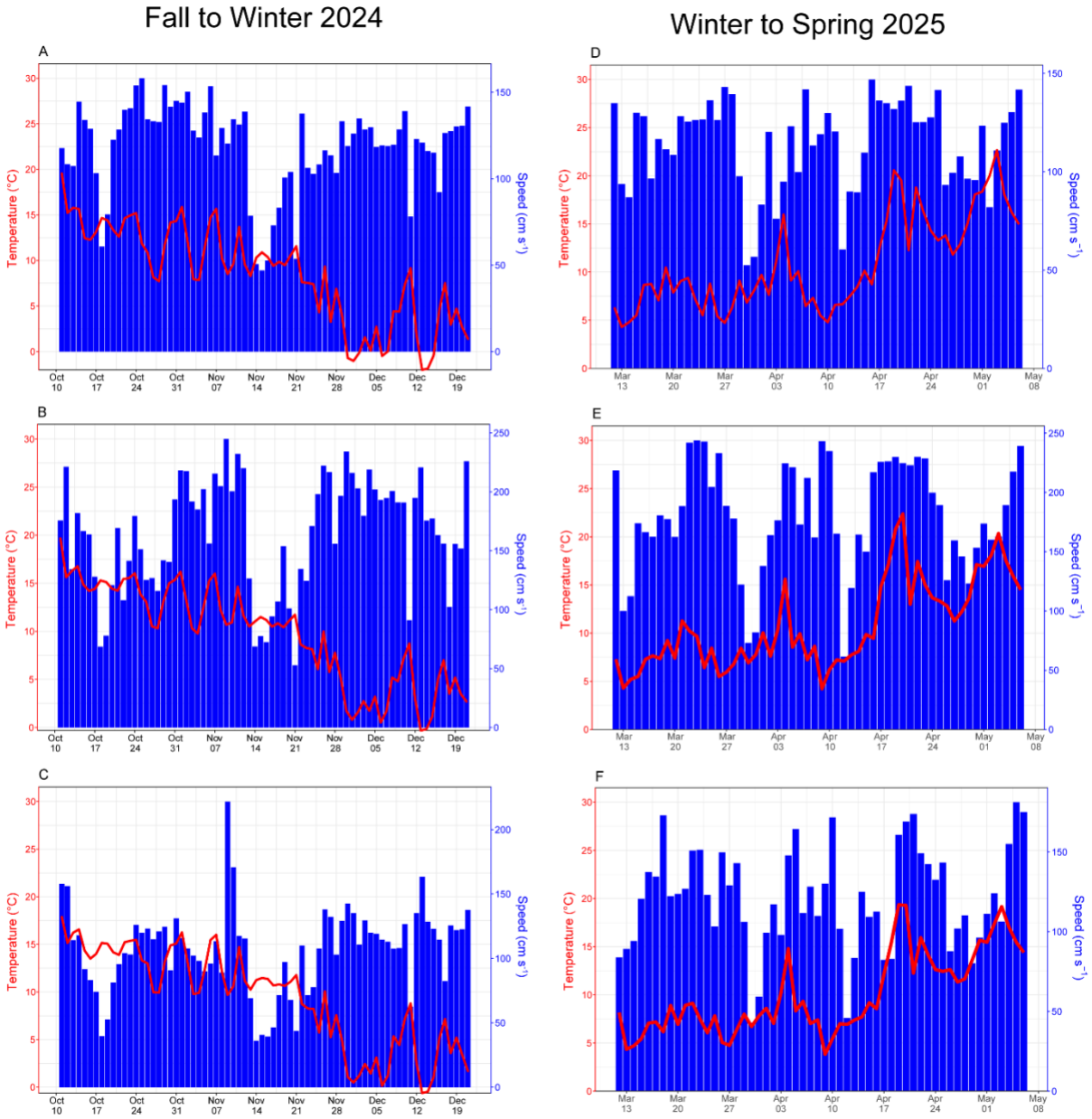

Figure 9. Gansevoort Peninsula Salt Marsh. Mean daily water velocities (cm s^{-1}) and temperatures (°C) at the inshore (Panels A, D), midshore (Panels B, E), and offshore locations (Panels C, F).

	Mean Daily Velocity (cm s^{-1})	Mean Daily Temperature (°C)	Point-sample water velocity (cm s^{-1})	Point-sample Temperature (°C)	Overall Mean Velocity (cm s^{-1})	Overall Mean Temperature (°C)
Inshore	46.9 ± 56.4 to 158.1 ± 27.8	-2.0 ± 1.1 to 19.5 ± 4.2	0 to 249	-6 to 27	106 ± 59.2	8.5 ± 5.9
Midshore	52.8 ± 77.2 to 244.8 ± 4.9	-0.3 ± 1.9 to 19.6 ± 3.5	0 to 249	-6 to 27	164 ± 81	9.6 ± 5.6
Offshore	36 ± 52.1 to 221.8 ± 18.7	-0.6 ± 2.1 to 17.9 ± 1.7	0 to 249	-6 to 27	118 ± 48.3	9.4 ± 5.7

Table 2a. *Fall and Winter 2024* Salt Marsh – Gansevoort Peninsula. Ranges and means with standard deviations of water properties at the inshore, midshore, and offshore meter locations.

The difference in overall mean water velocity among meter locations (Fig. 9a) in the salt marsh habitat was significant ($H = 1296.9$, $p < 0.001$) with the highest velocity at the midshore location (Table 2a; Fig. 10a). The difference in mean water temperature (°C) was also significant ($H = 74.384$, $p < 0.001$) among locations, albeit small at approximately ± 1°C with the highest temperature at the midshore location. (Table 2a; Fig. 10a).

	Mean Daily Velocity (cm s^{-1})	Mean Daily Temperature (°C)	Point-sample water velocity (cm s^{-1})	Point-sample Temperature (°C)	Overall Mean Velocity (cm s^{-1})	Overall Mean Temperature (°C)
Inshore	52.5 ± 68.4 to 150 ± 27.2	4.3 ± 1.8 to 22.7 ± 10.0	0 to 249	-1 to 39	114 ± 48.2	10.9 ± 7.0
Midshore	61.5 ± 86.2 to 244 ± 2.0	4.22 ± 7.5 to 22.4 ± 8.6	0 to 249	-2 to 40	180 ± 84.0	10.9 ± 7.3
Offshore	42.9 ± 59.3 to 181.2 ± 36.0	3.82 ± 6.1 to 19.4 ± 9.8	0 to 249	-6 to 27	121 ± 67.8	10.1 ± 6.3

Table 2b. *Winter and Spring 2025* Salt Marsh – Gansevoort Peninsula. Ranges and means with standard deviations of water properties at the inshore, midshore, and offshore meter locations.

The difference in overall mean water velocity among meter locations (Fig. 9b) in the salt marsh habitat was significant ($H = 1386$, $p < 0.001$) with the highest velocity at the midshore location (Table 2b; Fig. 10b). The difference in mean water temperature (°C) was also significant ($H = 14.433$, $p < 0.001$) among locations, albeit small at approximately ≤ 1°C with the highest temperatures at the inshore and midshore locations (Table 2b; Fig. 10b).

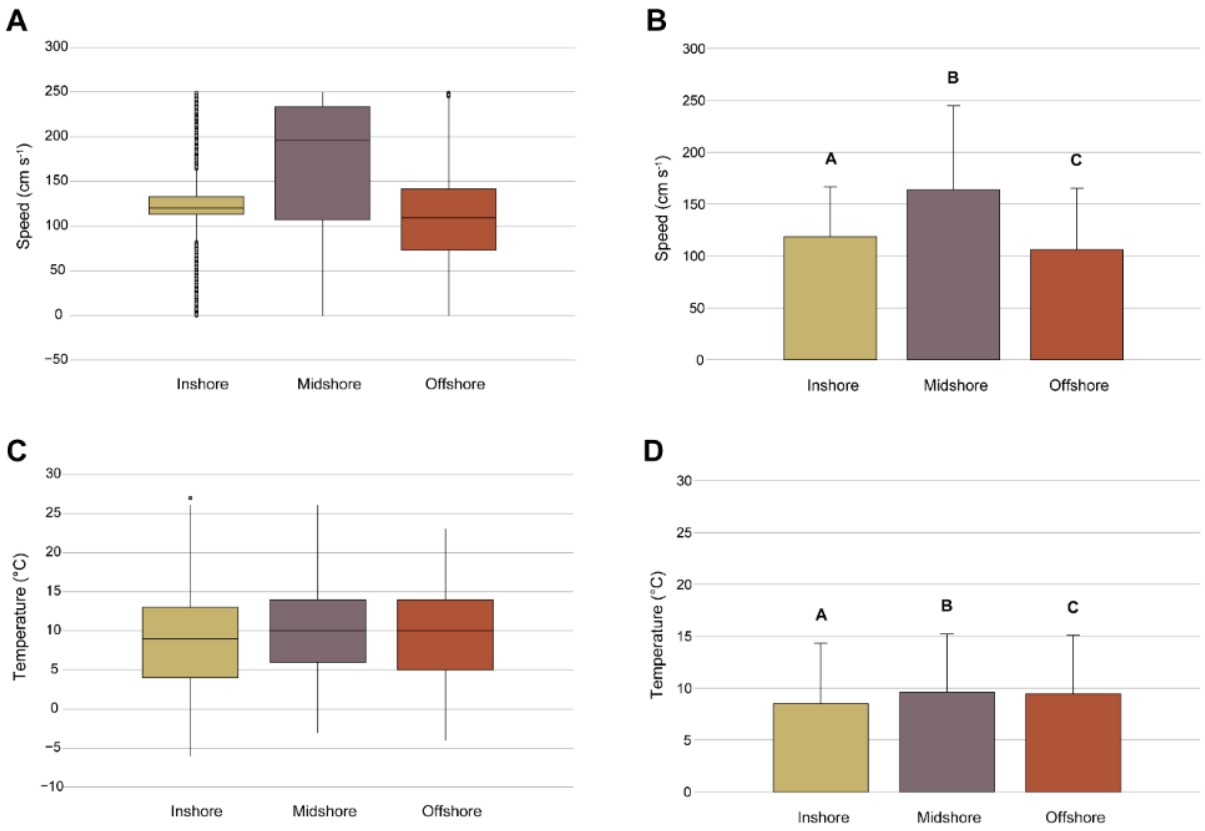

Figure 10a. *Fall and Winter 2024* Salt Marsh – Gansevoort Peninsula. Box-and-whisker plots showing the upper and lower adjacent values of the smallest and largest water velocity (cm s^{-1}) (Panel A) and temperature (°C) (Panel C) observations within the range (median – 1.5 IQR, median + 1.5 IQR), where IQR is the interquartile range; outliers are individual observations outside the range of adjacent values. Overall mean water velocity (cm s^{-1}) (Panel B) and temperature (°C) (Panel D); error bars are standard deviations.

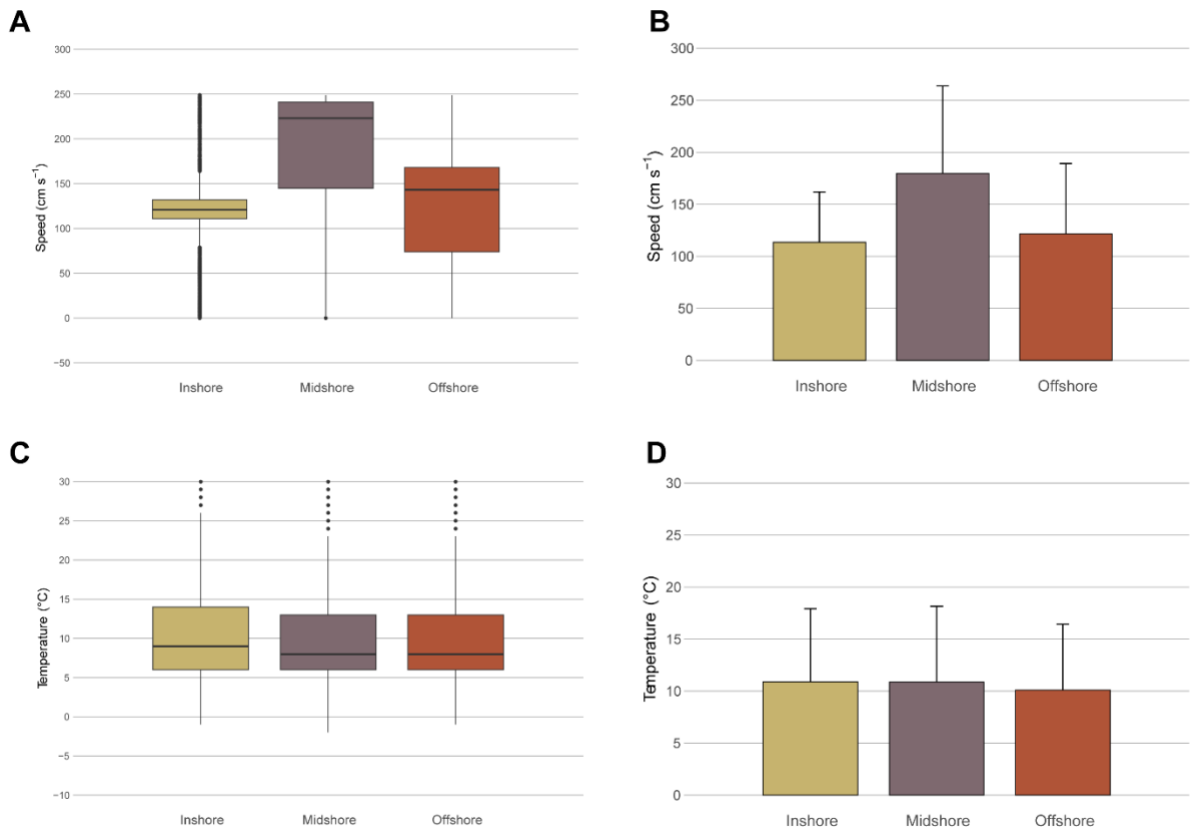

Figure 10b. *Winter and Spring 2025* Salt Marsh – Gansevoort Peninsula. Box-and-whisker plots showing the upper and lower adjacent values of the smallest and largest water velocity (cm s^{-1}) (Panel A) and temperature (°C) (Panel C) observations within the range (median – 1.5 IQR, median + 1.5 IQR), where IQR is the interquartile range; outliers are individual observations outside the range of adjacent values. Overall mean water velocity (cm s^{-1}) (Panel B) and temperature (°C) (Panel D); error bars are standard deviations.

Comparing water velocity and temperature through October, November, and December 2024, the difference in monthly water velocity (cm s^{-1}) was significant (H = 81.03, $p < 0.001$) and increased from October to December 2024 (Table 3; Fig. 11). Additionally, the difference in mean monthly water temperature (°C) was significant (H = 5440.3, $p < 0.001$) and decreased from October to December 2024 (Table 3; Fig. 11).

Month	Mean Daily Velocity (cm s^{-1})	Mean Daily Temperature (°C)
October	125 ± 67.3	14.1 ± 3.54
November	125 ± 74.9	10.0 ± 4.02
December	140 ± 59.4	2.96 ± 3.72

Table 3a. *Fall and Winter 2024* **Salt Marsh – Gansevoort Peninsula**. Monthly (October to December) overall mean water velocity (cm s^{-1}) and temperature (°C) with standard deviations.

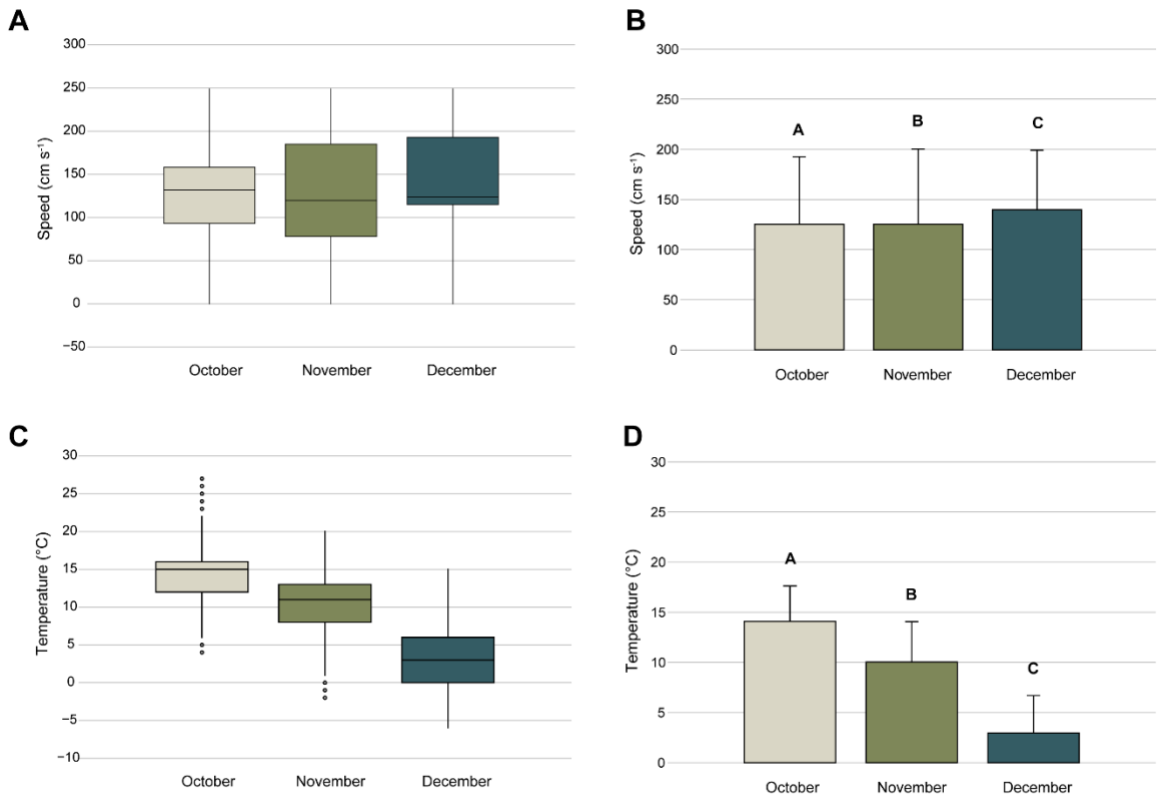

Figure 11a. *Fall and Winter 2024* Salt Marsh – Gansevoort Peninsula. Box-and-whisker plots showing the upper and lower adjacent values of the smallest and largest water velocity (cm s^{-1}) (Panel A) and temperature (°C) (Panel C) observations within the range (median – 1.5 IQR, median + 1.5 IQR), where IQR is the interquartile range; outliers are individual observations outside the range of adjacent values. Overall mean water velocity (cm s^{-1}) (Panel B) and temperature (°C) (Panel D); error bars are standard deviations.

Comparing water velocity and temperature through March, April, and May 2025, the difference in monthly water velocity (cm s^{-1}) was not significant (H = 1.8026, p = 0.406) and only slightly increased from March to May 2025 (Table 3b; Fig. 11b). Additionally, the difference in mean monthly water temperature (°C) was significant (H = 5440.3, p < 0.001) and increased from March to May 2025 (Table 3b; Fig. 11b).

Month	Mean Daily Velocity (cm s^{-1})	Mean Daily Temperature (°C)
March	134.7 ± 46.6	7.2 ± 1.7
April	138.9 ± 46.6	11.4 ± 4.24
May	150.5 ± 41	17.4 ± 2.2

Table 3b. *Winter and Spring 2025* **Salt Marsh – Gansevoort Peninsula**. Monthly (March to May) overall mean water velocity (cm s^{-1}) and temperature (°C) with standard deviations.

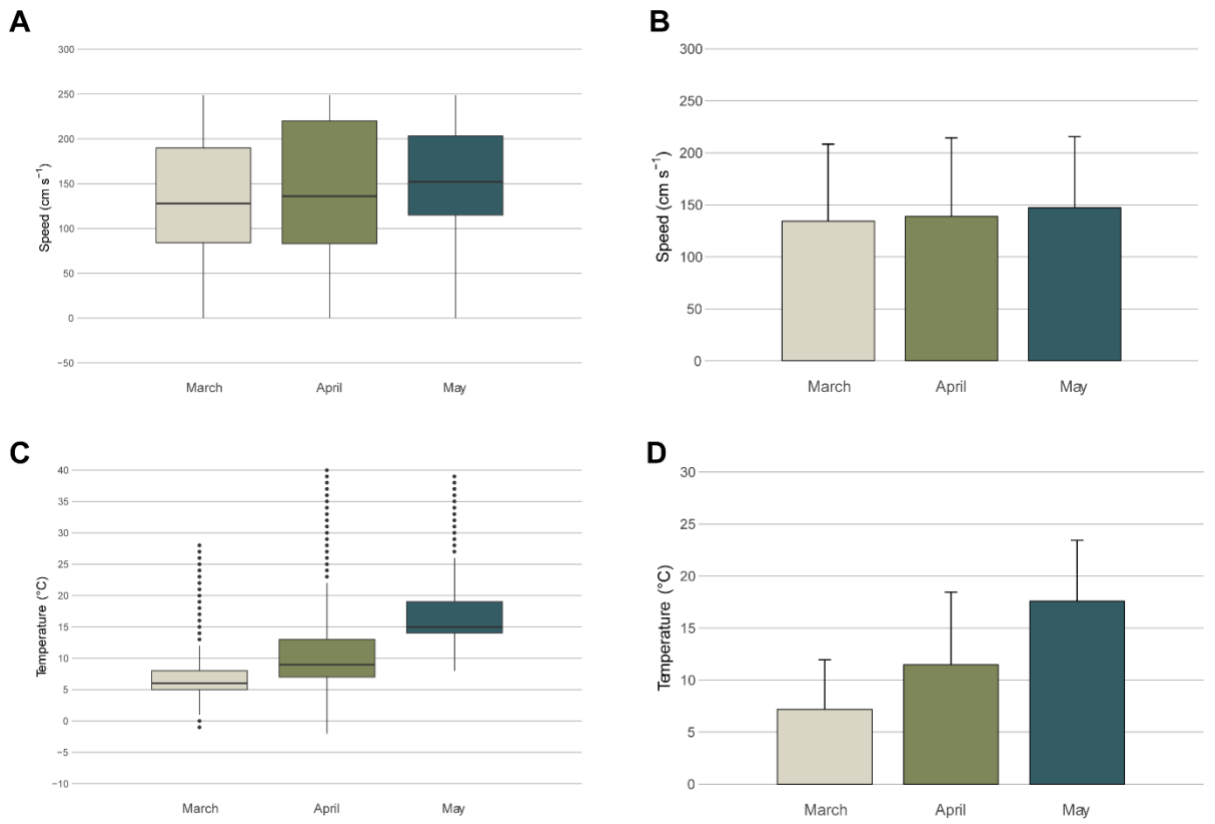

Figure 11b. *Winter and Spring 2025* Salt Marsh – Gansevoort Peninsula. Box-and-whisker plots showing the upper and lower adjacent values of the smallest and largest water velocity (cm s^{-1}) (Panel A) and temperature (°C) (Panel C) observations within the range (median – 1.5 IQR, median + 1.5 IQR), where IQR is the interquartile range; outliers are individual observations outside the range of adjacent values. Overall mean water velocity (cm s^{-1}) (Panel B) and temperature (°C) (Panel D); error bars are standard deviations.

NOAA tide predictions and water levels

In this study, we used water velocity (cm s^{-1}) and temperature (°C) data that were recorded within a six-hour window around high tide (referenced from the Mean Lower Low Water, MLLW) according to water level data collected at the NOAA tides and current station at the Battery (Station 8518750; NOAA's Center for Operational Products and Services, National Ocean Service). To test if the height of the water level (m) affected water velocity (cm s^{-1}), we analyzed data collected by Dr. Chester Zarnoch (Baruch College, CUNY) at Gansevoort Peninsula salt marsh using a field instrument deployed *in situ* between July and November 2024. Furthermore, to test if the tidal estimates from NOAA predictions corresponded with local water levels (m) at the salt marsh, we categorized water velocity measurements (cm s^{-1}) as high or low based on NOAA predictions. Using a locally estimated scatterplot smoothing analysis (LOESS), we showed an overlap of low and high tides (based on the NOAA predictions) equal to and below 0.02 m (Fig. 12). Although water velocity (cm s^{-1}) between the two tides at ≤ 0.02 m were similar (Fig. 13 and Table 4), a *t*-test showed a significant difference (p = 0.04) with low tide yielding a higher mean water velocity (cm s^{-1}). Further research will

be needed to confirm if wave velocity meters are fully submerged at 0.20 m water level at Gansevoort Peninsula salt marsh.

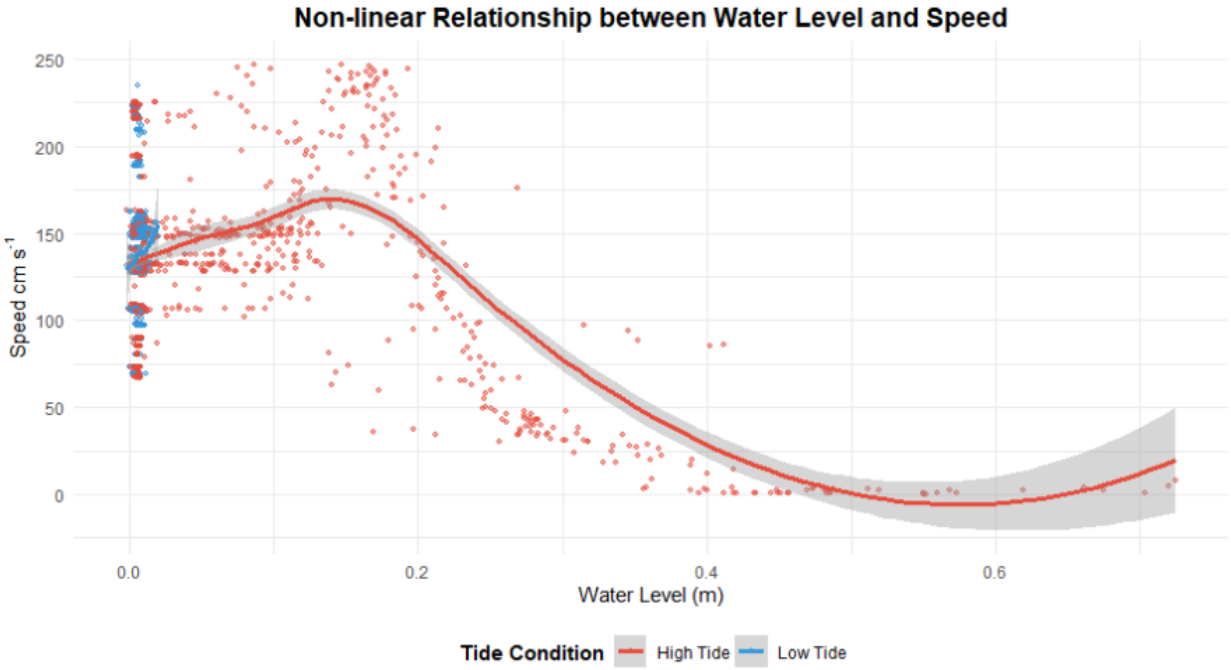

Figure 12. Locally estimated scatterplot smoothing analysis (LOESS) shows a nonlinear relationship between water level (m) and velocity (cm s^{-1}) at the Gansevoort Peninsula salt marsh.

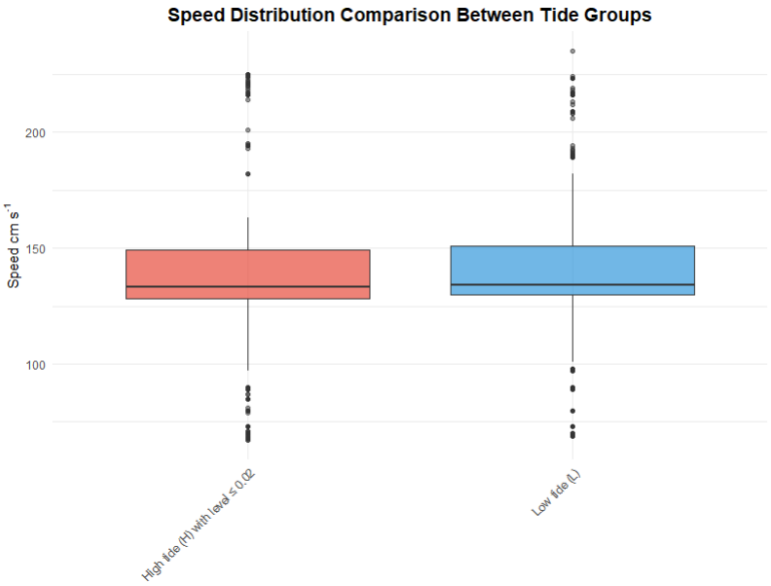

Figure 13. Box-and-whisker plots showing the upper and lower adjacent values of the smallest and largest water velocity (cm s^{-1}) observations within the range (median – 1.5 IQR, median + 1.5 IQR) at high and low tides equal to and below 0.02 m water level; IQR is the interquartile range and outliers are individual observations outside the range of adjacent values.

Tide	Mean Speed (cm s^{-1})	Minimum Speed (cm s^{-1})	Maximum Speed (cm s^{-1})
High tide: water level ≤ 0.02 m	134 ± 34	67	225
Low tide	134 ± 30	69	235

Table 4. Salt Marsh – Gansevoort Peninsula. Overall mean water velocity (cm s^{-1}) with standard deviations for high (≤ 0.02 m water level) and low tides.

Next, we implemented a critical water level threshold analysis by examining the precipitous and rapid decline in water velocity using derivatives of locally estimated scatterplot smoothing (LOESS) curves (Fig. 14). We defined a critical water level threshold at approximately 0.20 m where water velocity (cm s^{-1}) was greatly reduced during high tide conditions. Specifically, our results showed a 68.7% reduction across the 0.20 m primary threshold. At water levels (m) less than this threshold (< 0.18 m), the mean water velocity was 161.9 cm s^{-1} and decreased to 50.7 cm s^{-1} at water levels ≥ 0.20 cm. The maximum decline rate occurred at a water level of 0.22 m and represented an extreme response to tidal cycle. We defined the water level (m) transition zone of water velocity reduction to be 0.18 – 0.22 m.

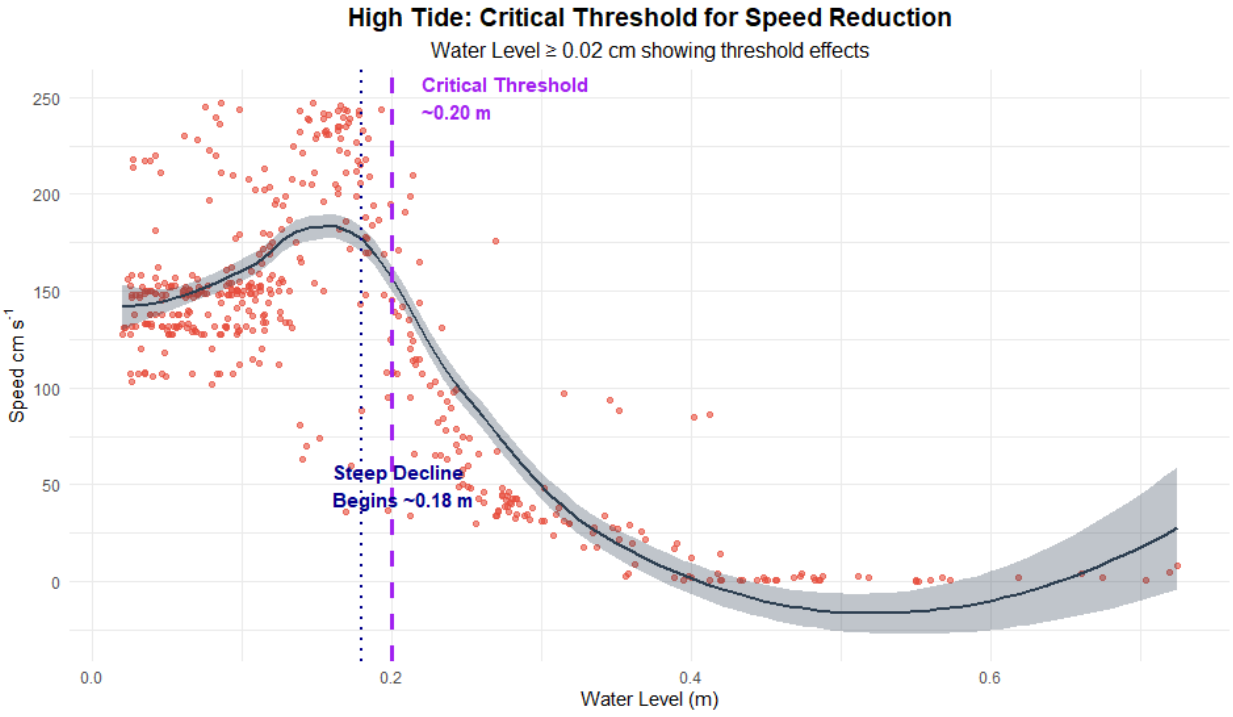

Figure 14. Figure 12. Locally estimated scatterplot smoothing analysis (LOESS) shows a nonlinear relationship between high tide water level (m) and velocity (cm s^{-1}) at the Gansevoort Peninsula salt marsh. A steep decline in water velocity (cm s^{-1}) was observed at ~0.18 m and critical threshold at ~0.20 m water level.

Discussion

We investigated the hyperlocal environmental heterogeneity of water velocity (cm s^{-1}) (a proxy for *wave exposure*) and temperature (°C) at intertidal and salt marsh habitats at Hudson River Park's Gansevoort Peninsula during Summer, Autumn, and Winter 2024 and late Winter and early Spring 2025. Our results show that water velocity (cm s^{-1}) along the rocky intertidal habitat was higher at the western location, towards the Hudson River channel, compared to the eastern location closer to Hudson River Park's esplanade. In the salt marsh habitat, although water temperature (°C) decreased from October to December in line with usual seasonal changes, we were surprised to find that water velocity differed along the short width of the salt marsh habitat, and that the highest water velocity (cm s^{-1}), on average, occurred in the center of the salt marsh. We attribute the increase in mean water velocity (cm s^{-1}) to environmental conditions that possibly covary with the change in seasons, and plan to investigate possible causative factors, such as the frequency and magnitudes of northwest winds and winter storms that may have affected the New York City metropolitan region from October to December 2024. Another possible explanation is the depression in the center of the marsh that was constructed to yield water flow to the revetments. As expected, water temperatures increased (°C) from late Winter through early Spring (March to May 2025).

Throughout this study, we used water velocity (cm s^{-1}) and temperature (°C) data that were recorded within a six-hour window around high tide according to water level data collected at the NOAA tides and current station at the Battery. To test if the height of the water level (m) affected water velocity (cm s^{-1}), we analyzed data collected by Dr. Chester Zarnoch (Baruch College, CUNY) at Gansevoort Peninsula salt marsh using a field instrument deployed *in situ* between July and November 2024. We showed an overlap of low and high tides (based on the NOAA predictions) equal to and below 0.02 m and identified a critical water level threshold at approximately 0.20 m where water velocity (cm s^{-1}) was greatly reduced during high tide conditions. Further research will be needed to confirm if wave velocity meters are fully submerged at 0.20 m water level at Gansevoort Peninsula salt marsh and recommend environmental monitoring use water velocity and level meters to identify how extreme increases and reductions in water motion affect the health and populations dynamics of cord grass.

We expect that after about 12 months of data collection, we will be able to apply advanced mathematical and statistical methods including Autocorrelation Analysis and Fourier Transform to tease out patterns and temporal trends. For example, to check the data under different assumptions of parameters and distributions, we will test hypotheses using generalized linear models (GLMs) and Bayesian fitting for one-way analysis of variance. In addition to the daily, monthly, and overall mean water velocity (cm s^{-1}) and temperature (°C), we are currently examining differences in the variation, outliers, and extreme values between locations and times. For example, we are currently analyzing the temporal trends in daily mean water velocities (cm s^{-1}) and temperatures (°C) to test whether observed spikes are part of a cyclical pattern or whether they occur randomly.

Future Directions

We have two main recommendations for continuing this research at Gansevoort. First, for monitoring water velocity at the salt marsh, wave meters should be paired with two or more onset water level meters to examine the water velocity at different tidal cycles more accurately. So far, we have assumed total submergence of meters at all high-tide cycles predicted by NOAA, which may not hold completely. Second, we recommend installing additional wave meters directly to the oyster gabions that are always submerged at all tide cycles/water levels, which may require the involvement of technical scuba divers

References

Brandon CM, Woodruff JD, Orton PM, Donnelly JP (2016) Evidence for elevated coastal vulnerability following large-scale historical oyster bed harvesting. Earth Surf Processes Landf 41:1136–1143

Cowardin LM, Fish US, Carter V, Golet FC (1979) Classification of wetlands and deepwater habitats of the United States.

Denny MW (1988) Biology and the mechanics of the wave-swept environment. Princeton University Press, Princeton, N.J.

Denny MW, Gaylord B (2010) Marine Ecomechanics. Annu Rev Mar Sci 2:89–114

Feagin RA, Lozada-Bernard SM, Ravens TM, Möller I, Yeager KM, Baird AH (2009) Does vegetation prevent wave erosion of salt marsh edges? Proc Natl Acad Sci USA 106:10109–10113

Fitzgerald AM, Wallace WG, Zarnoch CB (2020) Spatial and temporal trends in physiological biomarkers of adult eastern oysters, Crassostrea virginica, within an urban estuary. Marine Environmental Research 161:105122

Karimpour A, Chen Q, Twilley RR (2017) Wind Wave Behavior in Fetch and Depth Limited Estuaries. Sci Rep 7:40654

Lenihan HS, Peterson CH (1998) How habitat degradation through fishery disturbance enhances impacts of hypoxia on oyster reefs. Ecological Applications 8:128–140

Lenihan HS (1999) Physical-Biological Coupling on Oyster Reefs: How Habitat Structure Influences Individual Performance. Ecol. Monog 69(3):251–275

Massel SR (1999) Fluid mechanics for marine ecologists. Springer, Berlin

Sousa WP (1984) The Role of Disturbance in Natural Communities. Annu Rev Ecol Syst 15:353–391

Zarnoch CB, Schreibman MP Growth and Reproduction of Eastern Oysters, Crassostrea Virginica, in a New York City Estuary: Implications for Restoration.

Zedler JB, Kercher S (2005) WETLAND RESOURCES: Status, Trends, Ecosystem Services, and Restorability. Annu Rev Environ Resour 30:39–74